metals

MDPI

Article

Influence of Milling Atmosphere on the Controlled Formation of Ultrafine Dispersoids in Al-Based MMCs

Eduardo S. Caballero [1], Jesús Cintas [1], Francisco G. Cuevas [2,*], Juan Manuel Montes [1] and Fátima Ternero [1]

[1] Metallurgy and Materials Engineering Group, Escuela Técnica Superior de Ingeniería, Universidad de Sevilla, Camino Descubrimientos s/n, Sevilla 41092, Spain; esanchez3@us.es (E.S.C.); jcintas@us.es (J.C.); jmontes@us.es (J.M.M.); fternero@us.es (F.T.)

[2] Department of Chemical Engineering, Physical Chemistry and Materials Science, Escuela Técnica Superior de Ingeniería, Universidad de Huelva, La Rábida, Carretera Palos s/n, Huelva 21819, Spain

* Correspondence: fgcuevas@dqcm.uhu.es; Tel.: +34-959-217-448

Academic Editor: Chun-Liang Chen
Received: 27 July 2016; Accepted: 8 September 2016; Published: 12 September 2016

Abstract: Properties of compacts made from aluminium powder, milled under different atmospheres, were evaluated. The duration of all the milling processes was 10 h, although different atmospheres were tested: vacuum, confined ammonia, and vacuum combined with a short-time ammonia gas flow (5 min). Milled powders were consolidated by cold uniaxial pressing and vacuum sintering.The nature and content of the second phases change with the milling atmosphere, allowing the modification of the mechanical properties of the compacts. Results showed that hardness and tensile strength were highly dependent on the milling atmosphere. Milling carried out in vacuum with a short-time ammonia gas flow notably improved compacts' properties, as compared with 10 h vacuum milling. Hardness increased from 96 to 150 HB, and ultimate tensile strength rose from 247 to 476 MPa.

Keywords: Al-based MMCs; milling; sintering; N-base dispersoids

1. Introduction

Weight saving is a main aim in the automotive and aerospace industries. Increasing the use of lightweight alloys (e.g., aluminium) leads to a significant reduction in the overall weight, fuel consumption, and pollution of automobiles and aircrafts [1–4]. Aluminium has a very low density (2.7 g/cm^3), high specific strength, excellent low temperature performance, good formability, and exceptional corrosion resistivity [5,6]. Despite their interesting properties, commercial heat-treated aluminium alloys suffer a remarkable degradation of properties at high temperature. Traditionally, the strengthening of aluminium alloys has been obtained by precipitation hardening, resulting in a homogeneous dispersion of fine intermetallic particles [7]. However, these particles are not able to avoid the degradation of mechanical properties at high temperatures [8], since their metallic nature promotes a rapid grain growth and an overaging of the alloy. To overcome these problems, aluminium alloys can be reinforced by hard ceramic particles to produce aluminium matrix composites (AMCs).

AMCs are low-weight and high-performance materials that have attracted considerable attention in many advanced applications in railway transport systems, the aerospace industry, and in armoured vehicles [9,10]. Owing to their excellent physical and mechanical properties, AMCs have the potential to replace conventional materials in the automobile and aircraft industries. The properties of AMCs can be tailored by changing the fraction, size, and type of reinforcing particles [11–14]; it is possible to add

oxides (Al_2O_3 or Y_2O_3), carbides (SiC or TiC), nitrides (AlN), and borides (TiB_2 or B_4C), among many others [15–18].

Obtaining AMCs with excellent properties requires the successful incorporation of ceramic particles with a good bonding with the aluminium matrix. Several methods in solid and liquid states have been developed for the dispersion of fine particles [19–22]. In liquid methods, the entire aluminium matrix is melted, and the ceramic particles are gradually introduced into the molten aluminium by stirring before casting. These methods are widely used due to their simplicity, although the resulting distribution is generally inhomogeneous. Conversely, the solid-state route ensures a uniform distribution of reinforcement particles in the matrix. In this regard, the powder metallurgy (PM) process allows aluminium powder and reinforcement particles to be mixed at room temperature. In the powder metallurgy field, aluminium has traditionally been reinforced with directly-added ceramic particles [23–27]. However, another way to strengthen aluminium alloys by a homogeneous distribution of fine particles has been developed. Thus, it is known that mechanical alloying (MA) allows solid–gas reactions to take place between powder and milling atmosphere at room temperature, or at least at much lower temperatures than are normally required [28–30].

The aim of this work is to develop a new aluminium base material with better mechanical properties than commercial alloys. To attain this objective, as-received aluminium powder (AR Al) was milled in a combined atmosphere of vacuum and a short-time ammonia gas flow. This combination was used in order to achieve precise control over the dispersion of fine refractory formed particles (mainly nitrides). After milling, aluminium matrix composites (AMCs) were produced by uniaxial cold pressing and vacuum sintering

2. Experimental Procedure

The starting material (AR Al) was atomized elemental aluminium powder (AS 61, Eckart) with a purity level higher than 99.7% and a mean particle size of 80.5 μm. A high-energy attritor ball-mill was used to process the aluminium powder for 10 h. Different atmospheres were tested: vacuum (V), confined ammonia (A), and vacuum followed by 5 min ammonia gas flow (AF-5). In this last case, ammonia was incorporated after 2 h of milling, and then millings continued in vacuum until reaching 10 h. The ammonia gas purity was higher than 99.96% (Air Liquide). The water-cooled stainless steel vessel had a capacity of 1400 cm^3. Etilen bis-stereamide (EBS) micropowder organic wax (3 wt %) was used as a process control agent (PCA) during milling. Mill charge contained 72 g of powder and 3600 g of balls (charge ratio 50:1). All millings were carried out with a rotor speed of 500 rpm, at room temperature, for a total time of 10 h.

After powder milling, granulometry and morphology were analysed by laser diffraction (Mastersizer 2000, Malvern, Worcestershire, UK) and scanning electron microscopy (SEM XL-30, Philips, Amsterdam, The Netherlands), respectively. Powders were consolidated by cold uniaxial pressing (850 MPa, 2 min hold time, using EBS wax as die-wall lubricant) and vacuum (5 Pa) sintering (650 °C, 1 h), followed by furnace cooling. The sintering ramp used was: 10 °C/min up to 600 °C, followed by 5 °C/min up to 645 °C, and finally, 1 °C/min up to 650 °C, which was kept for 1 h. Both cylindrical (diameter: 12 mm; mass: ca. 4 g) and "dog-bone" shape [31] compacts (32 mm × 4 mm × 4 mm) were produced, and 15 samples of each geometry were tested for the three materials studied. X-ray diffraction analysis (XRD, Bruker D8 Advance, CuKα radiation) was carried out on powders, and also on compacts, to identify the phases formed both before and during sintering. The microstructure of the sintered compacts were also studied by transmission electron microscopy (TEM Talos F200, FEI, Hillsboro, OR, USA). Compacts' density, hardness (Emco-M4U-025), and tensile strength and elongation (Instron 5505) were evaluated.

3. Results and Discussion

The densification ability of milled powders under different atmospheres was firstly studied. It is well known in the powder metallurgy field that densification ability is strongly influenced by different

factors: powder hardness, particle morphology, mean particle size, as well as their size distribution. The last two factors were determined from granulometric characterization. Because of the relatively long milling (10 h), all milled powders exhibited a similar granulometric distribution, with a mean particle size around 20 μm (Figure 1).

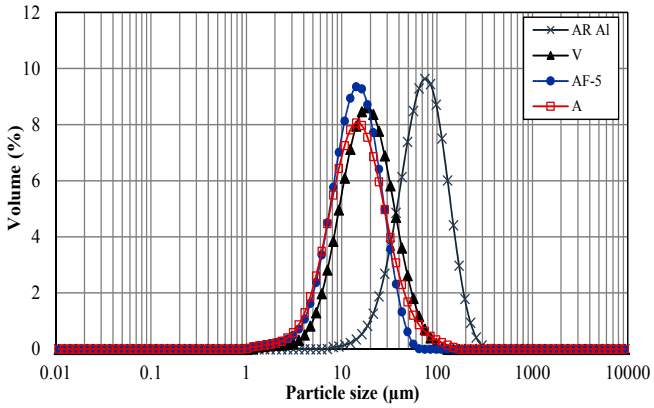

Figure 1. Granulometric distribution of milled powders. A: confined ammonia; AF-5: vacuum followed by 5 min ammonia gas flow; AR Al: as-received aluminum powder; V: vacuum.

On the other hand, particle morphology was studied by SE-SEM (secondary electrons SEM). Results show that all milled powders tended to an equiaxial morphology. Figure 2 collects SEM micrographs corresponding to vacuum (V) milled powders and powders milled in confined NH_3 (A), that of the AF-5 powder being very similar. The combination of a reduced particle size together with an equiaxial geometry suggests that a high relative density can be achieved.

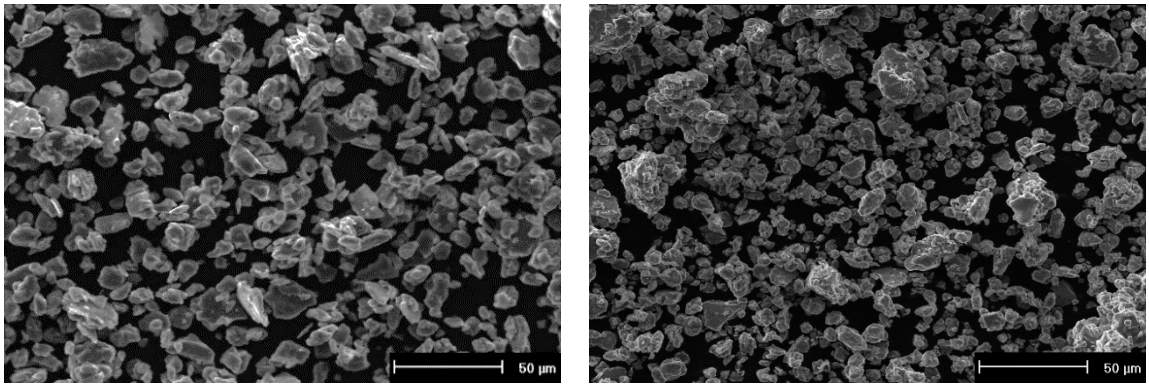

(**a**) (**b**)

Figure 2. SE-SEM micrographs of (**a**) V and (**b**) A powders.

In this way, a compressibility test (Figure 3a) was carried out in order to measure the relative green density versus the applied compaction pressure, as well as to indirectly estimate the hardness of the powders; the lower the relative density, the higher the powder hardness. Results show that densification ability is almost the same for powders milled in vacuum or in ammonia (confined or in flow). Thus, all powders reach relative densities above 90% for compaction pressures of about 850 MPa or higher. Since all milling experiments were carried out for the same total time of ten hours, the strain hardening of the aluminium powders should be the same in all of them. Therefore, the presence of ammonia gas during the milling process only provoked a slight hardening of aluminium powders with respect to those that are mechanically alloyed in vacuum. This small increase in hardening is due to nitrogen incorporation into the aluminium lattice in solid solution [32].

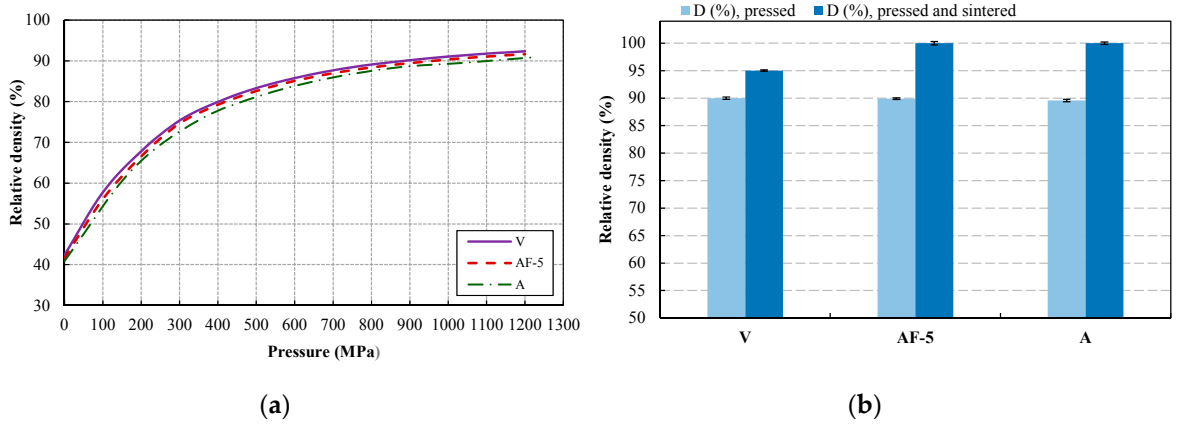

(**a**) (**b**)

Figure 3. (**a**) Compressibility curves of mechanically alloyed aluminium powders and (**b**) relative density after being pressed and sintered.

On the other hand, Figure 3b shows the relative density of the different compacts, both after being pressed (850 MPa) and after being sintered (650 °C, 1 h). As can be observed, the relative density of green compacts is almost the same (90%), which is congruent with the compressibility curves. After sintering, the relative density of V compacts decreased, reaching a value of 95%. On the contrary, a relative density close to 100% was reached in sintered compacts from powders milled under ammonia gas (AF-5 and A). Therefore, the ability to densify is improved by the presence of ammonia gas. Thus, a high level of porosity (10%) is eliminated during sintering in compacts from powders milled in ammonia, compared vacuum milled powder compacts.

Obviously, the effect of ammonia gas on the milled powder must also affect to the mechanical behaviour of compacts made from them. In this way, tensile behaviour (ultimate tensile strength, UTS, and elongation, E) and hardness (HB) were evaluated on "dog-bone" and cylindrical shape compacts, respectively.

Figure 4 shows an increase of UTS values from 302 MPa, corresponding to V compacts, up to 476 and 489 MPa for AF-5 and A compacts, respectively. Despite a slightly higher UTS being reached with confined ammonia (A), the results corresponding to elongation show that it is more effective to incorporate a short-time ammonia gas flow during milling in vacuum. In any case, both UTS and elongation values are higher when milling is carried out in the presence of ammonia gas (AF-5 and A). This can be due to two factors: firstly, the low porosity achieved after sintering (Figure 3b) in compacts from powders milled in ammonia reduces tension concentrators, so that UTS is improved whereas elongation is kept or even increases; and on the other hand, the possible formation of second phases in the aluminium matrix as result of solid solution hardening from NH_3 gas may have a remarkable influence on mechanical properties. Effectively, TEM images corresponding to V and AF-5 sintered compacts (Figure 5) show the presence of nanosized phases finely dispersed in the matrix. However, results indicate that the strengthening is more efficient when compacts are made from powder milled under ammonia gas (AF-5 and A) compared to compacts powder milled in vacuum (V).

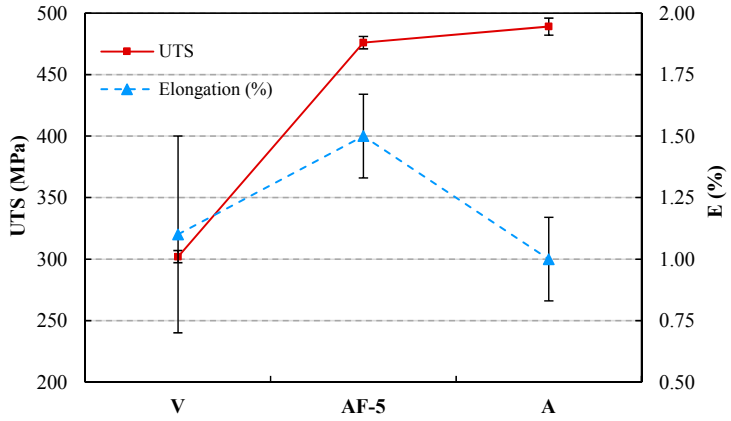

Figure 4. Ultimate tensile strength (UTS) and elongation (E) of sintered compacts.

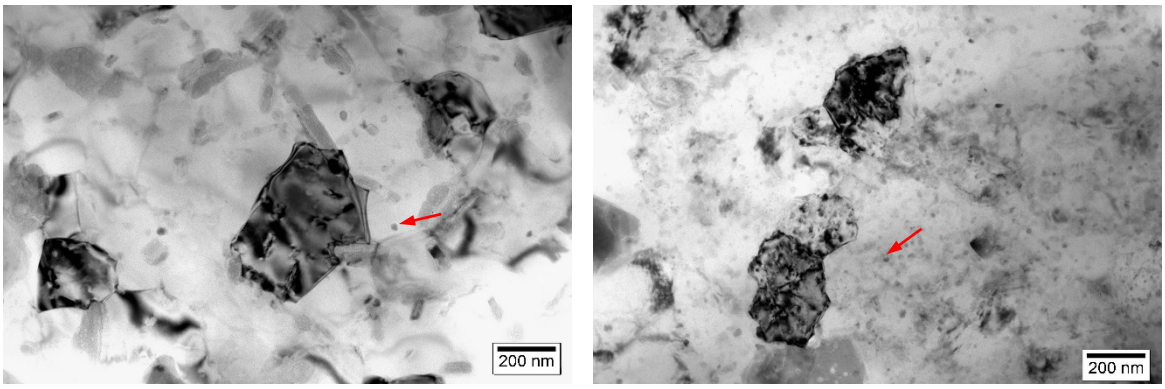

(**a**) (**b**)

Figure 5. TEM micrograph showing aluminium grains and nanosized dispersoids (arrows) in (**a**) V and (**b**) AF-5 sintered compacts.

Figure 6 shows that reflections corresponding to aluminium carbide (Al_4C_3) and aluminium oxide (Al_2O_3) were detected in all sintered samples. However, reflections corresponding to nitrogen-rich second phases (Al_4CON and Al_5O_6N) were also observed in compacts powder milled with ammonia gas (AF-5 and A). During the milling process, aluminium particles react with the carbon and oxygen coming from the organic wax used as PCA, as well as with the nitrogen arising from the ammonia gas dissociation, with only aluminium peaks being detected in as-milled powders because a solid solution is formed. In this way, the Al_4C_3, Al_3CON, and Al_5O_6N phases are formed during the subsequent sintering step [32]. On the other hand, the presence of aluminium oxide (Al_2O_3) comes from the oxide layers covering the surface of aluminium particles, while hydrogen is lost during the process.

In a similar way to UTS values, hardness is also expected to increase because of the incorporation of ammonia gas to the milling atmosphere. As observed in Figure 7, hardness values as high as 150 HB were obtained when ammonia gas was involved in mechanical alloying (AF-5 and A), being lower than 100 HB when milling was carried out only in vacuum. Furthermore, the hardness improvement was more effective in the case where a short-time ammonia gas flow was used, instead of a confined ammonia atmosphere. It has been proven that the ability to incorporate nitrogen to the aluminium lattice is much higher when milling starts in vacuum [33]. This high reactivity is also revealed by the fact that AF-5 and A compacts reach almost the same UTS and hardness in spite of the considerable difference in time under ammonia gas. Moreover, ammonia flow implies a continuous supply of renewed gas, contrary to the confined ammonia atmosphere. Thus, compact hardness can be modified by controlling the atmosphere during mechanical alloying.

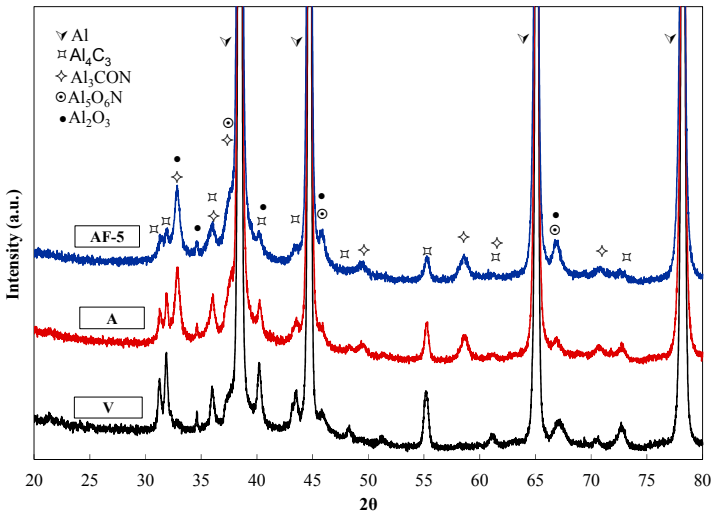

Figure 6. X-ray diffraction patterns of mechanically alloyed Al powders after sintering.

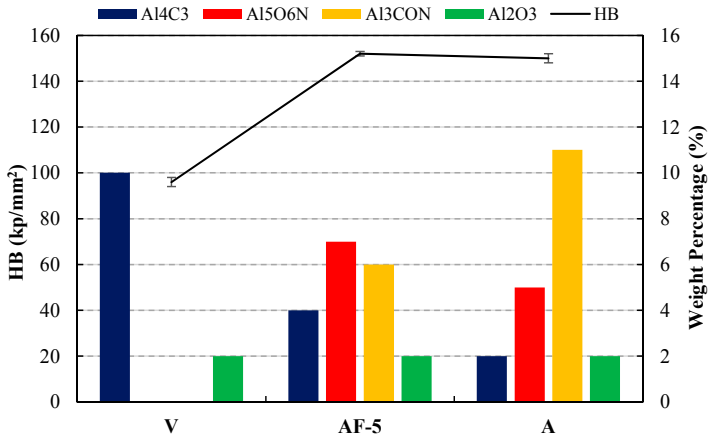

Figure 7. Hardness and weight percentage of the second phases formed in the different sintered samples.

As discussed above, the hardness of a PM sintered compact is influenced by the compact porosity and the hardness of the constituent particles. Compacts prepared with AF-5 and A powders reached a relative density near 100% after being sintered. Therefore, the hardness of such compacts is only due to the hardness of the powder particles. The aforementioned strain hardening is the same for all millings, so hardness and UTS differences must be produced by the presence of hard phases dispersed in the compacts, which are formed during sintering. Regarding the latter, XRD patterns were fitted via Rietveld refinement [34] to quantify the phases formed after sintering. An increase in the weight percentage of dispersoids from 12% up to 20% when ammonia gas was used during milling was observed (Figure 7). Furthermore, the amount of oxynitride and, mainly, oxycarbonitride aluminium (Al_5O_6N and Al_3CON, respectively) increased with the amount of time that ammonia gas was incorporated to the milling process, while that of aluminium carbide (Al_4C_3) decreased compared to vacuum milling (V). Likewise, the increase of the weight percentage of Al_3CON was much faster if ammonia gas was flowed rather than under confined conditions. It can be observed that only five minutes of ammonia flow allowed a weight percentage of second phases as high as in confined conditions during ten hours to be achieved.

Therefore, ammonia gas allows the formation of significant amounts of nanocrystalline dispersoids, having the previously described remarkable influence on the mechanical properties. Thereby, a better combination of mechanical properties is achieved by using a short-time ammonia

flow (AF-5) instead of confined conditions (A). In this regard, it is important to note that the mechanical properties reached are higher than those of the widely-used commercial alloys 2024-T4 (469 MPa and 120 HB) and 6061-T6 (310 MPa and 95 HB) at room temperature [35]. That is, when ammonia gas is incorporated as short-time flow instead of as confined atmosphere, the mechanical properties are similar, despite the fact that time under such gas is shorter.

4. Conclusions

Aluminium compacts made from powders mechanically alloyed in vacuum, confined ammonia, or vacuum in combination with a short-time ammonia gas flow were characterized.

The following conclusions are drawn:

(1) Ammonia gas improves the ability of powders to densify during sintering, reaching a density near 100%.

(2) Compacts from powder milled in vacuum are only reinforced by Al_4C_3 and Al_2O_3. However, milling with ammonia gas allows the formation of significant amounts of other nanocrystalline dispersoids (Al_4CON and Al_5O_6N), having a high influence on the improved mechanical properties of sintered compacts.

(3) A remarkable improvement on mechanical properties is achieved when a mechanical alloying process is carried out with ammonia, both confined and with a short-time flow. Furthermore, it has been noted that a short-time ammonia gas flow is more efficient than a confined atmosphere, since a deeper control of the mechanical properties may be achieved.

(4) The use of an ammonia gas flow of 5 min allows hardness and UTS values as high as with a confined ammonia atmosphere to be reached (150 HB and 476 MPa), despite the fact that ammonia gas consumption is much lower (0.3 L for AF-5 versus 1.85 L for A). Furthermore, under flowing gas, a greater elongation is achieved.

Acknowledgments: Financial support of the Ministerio de Economía y Competitividad (Spain) through the research projects DPI2015-69550-C2-1-P and DPI2015-69550-C2-2-P is gratefully acknowledged. We also thank the Microscopy Service of CITIUS (University of Seville).

Author Contributions: E.S. Caballero and J. Cintas conceived and designed the experiments; F.G. Cuevas and J. Montes performed the experiments; F. Ternero analyzed the data; E.S caballero, J. Cintas and F.G. Cuevas wrote the paper.

Conflicts of Interest: The authors declare no conflict of interest.

References

1. Dursun, T.; Soutis, C. Recent developments in advanced aircraft aluminium alloys. *Mater. Des.* **2014**, *56*, 862–871. [CrossRef]
2. Charitidis, C.A.; Dragatogiannis, D.A.; Koumoulos, E.P.; Kartsonakis, I.A. Residual stress and deformation mechanism of friction stir welded aluminum alloys by nanoindentation. *Mater. Sci. Eng. A* **2012**, *540*, 226–234. [CrossRef]
3. Srivastava, N.; Chaudhari, G.P. Strengthening in Al alloy nano composites fabricated by ultrasound assisted solidification technique. *Mater. Sci. Eng. A* **2016**, *651*, 241–247. [CrossRef]
4. Surappa, M.K. Aluminium matrix composites: Challenges and opportunities. *Sadhana* **2003**, *28*, 319–334. [CrossRef]
5. Xiang, N.; Song, R.; Zhao, J.; Li, H.; Wang, C.; Wang, Z. Microstructure and mechanical properties of ceramic coatings formed on 6063 aluminium alloy by micro-arc oxidation. *Trans. Nonferr. Met. Soc. China* **2015**, *25*, 3323–3328. [CrossRef]
6. Lipińska, M.; Bazarnik, P.; Lewandowska, M. The influence of severe plastic deformation processes on electrical conductivity of commercially pure aluminium and 5483 aluminium alloy. *Arch. Civ. Mech. Eng.* **2016**, *16*, 717–723. [CrossRef]
7. Ding, L.; Jia, Z.; Zhang, Z.; Sanders, R.E.; Liu, Q.; Yang, G. The natural aging and precipitation hardening behaviour of Al-Mg-Si-Cu alloys with different Mg/Si ratios and Cu additions. *Mater. Sci. Eng. A* **2015**, *627*, 119–126. [CrossRef]

8. Wierzbińska, M.; Sieniawski, J. The degradation of microstructure of $AlCu_4Ni_2Mg$ aluminium alloy after prolonged annealing at elevated temperature. *Solid State Phenom.* **2012**, *186*, 315–318. [CrossRef]
9. Abdoli, H.; Salahi, E.; Farnoush, H.; Pourazrang, K. Evolutions during synthesis of Al–AlN-nanostructured composite powder by mechanical alloying. *J. Alloy. Compd.* **2008**, *461*, 166–172. [CrossRef]
10. Feng, Y.; Chen, J.; Qiang, W.; Wang, K. Microstructure and mechanical properties of aluminium alloy 7A52 thick plates welded by robotic double-sided coaxial GTAW process. *Mater. Sci. Eng.* **2016**, *673*, 8–15. [CrossRef]
11. Mazahery, A.; Shabani, M.O. A comparative study on abrasive wear behavior of semisolid–liquid processed Al–Si matrix reinforced with coated B4C reinforcement. *Trans. Indian Inst. Met.* **2012**, *65*, 145–154. [CrossRef]
12. Cöcen, U.; Önel, K. Ductility and strength of extruded SiCp/aluminium-alloy composites. *Compos. Sci. Technol.* **2002**, *62*, 275–282. [CrossRef]
13. Cintas, J.; Cuevas, F.G.; Montes, J.M.; Herrera, E.J. Microstructural control of sintered mechanically alloyed Al-1%Ni material. *Scr. Mater.* **2005**, *52*, 341–345. [CrossRef]
14. Cintas, J.; Montes, J.M.; Cuevas, F.G.; Gallardo, J.M. Influence of PCA content on mechanical properties of sintered MA aluminium. *Mater. Sci. Forum* **2006**, *514–516*, 1279–1283. [CrossRef]
15. Chen, W.; Liu, Y.; Yang, C.; Zhu, D.; Li, Y. (SiCp+Ti)/7075Al hybrid composites with high strength and large plasticity fabricated by squeeze casting. *Mater. Sci. Eng. A* **2014**, *609*, 250–254. [CrossRef]
16. Kumar, C.; Rajadurai, J. Influence of rutile (TiO_2) content on wear and microhardness characteristics of aluminium-based hybrid composites synthesized by powder metallurgy. *Trans. Nonferr. Met. Soc. China* **2016**, *26*, 63–73. [CrossRef]
17. Sharma, P.; Sharma, S.; Khanduja, D. Production and some properties of Si_3N_4 reinforced aluminium alloy composites. *J. Asian Ceram. Soc.* **2015**, *3*, 352–359. [CrossRef]
18. Ostad Shabani, M.; Mazahery, A. Fabrication of AMCs by spray forming: Setting of cognition and social parameters to accelerate the convergence in optimization of spray forming process. *Ceram. Int.* **2013**, *39*, 5271–5279. [CrossRef]
19. Karabulut, S.; Gökmen, U.; Cinici, H. Study on the mechanical and drilling properties of AA7039 composites reinforced with $Al_2O_3/B_4C/SiC$ particles. *Compos. Part B Eng.* **2016**, *93*, 43–55. [CrossRef]
20. Chen, C.-L.; Lin, C.-H. Effect of Y_2O_3 and TiC reinforcement particles on intermetallic formation and hardness of Al6061 composites via mechanical alloying and sintering. *Metall. Mater. Trans. A* **2015**, *46*, 3687–3695. [CrossRef]
21. Mathan Kumar, N.; Senthil Kumaran, S.; Kumaraswamidhas, L.A. High temperature investigation on EDM process of Al 2618 alloy reinforced with Si_3N_4, AlN and ZrB_2 in-situ composites. *Alex. Eng. J.* **2016**, *663*, 755–768. [CrossRef]
22. Rengasamy, N.V.; Rajkumar, M.; Kumaran, S.S. Mining environment applications on Al 4032—Zrb_2 and Tib_2 in-situ composites. *J. Alloy. Compd.* **2016**, *658*, 757–773. [CrossRef]
23. Fogagnolo, J.B.; Robert, M.H.; Torralba, J.M. Mechanically alloyed AlN particle-reinforced Al-6061 matrix composites: Powder processing, consolidation and mechanical strength and hardness of the as-extruded materials. *Mater. Sci. Eng. A* **2006**, *426*, 85–94. [CrossRef]
24. Gasem, Z.M.; Ali, S.S. Low-cycle fatigue behavior of powder metallurgy 6061 aluminum alloy reinforced with submicron-scale Al_2O_3 particles. *Mater. Sci. Eng. A* **2013**, *562*, 109–117. [CrossRef]
25. Chen, Z.; Tokaji, K. Effects of particle size on fatigue crack initiation and small crack growth in SiC particulate-reinforced aluminium alloy composites. *Mater. Lett.* **2004**, *58*, 2314–2321. [CrossRef]
26. Karbalaei Akbari, M.; Baharvandi, H.R.; Shirvanimoghaddam, K. Tensile and fracture behavior of nano/micro TiB_2 particle reinforced casting A356 aluminum alloy composites. *Mater. Des.* **2015**, *66*, 150–161. [CrossRef]
27. Yang, H.; Topping, T.D.; Wehage, K.; Jiang, L.; Lavernia, E.J.; Schoenung, J.M. Tensile behavior and strengthening mechanisms in a submicron B_4C-reinforced Al trimodal composite. *Mater. Sci. Eng. A* **2014**, *616*, 35–43. [CrossRef]
28. Tweed, J.H. Manufacture of 2014 aluminium reinforced with SiC particulate by vacuum hot pressing. *Mater. Sci. Eng. A* **1991**, *135*, 73–76. [CrossRef]
29. Cintas, J.; Cuevas, F.G.; Montes, J.M.; Caballero, E.S.; Herrera, E.J. Strengthening of ultrafine PM aluminium using nano-sized oxycarbonitride dispersoids. *Mater. Sci. Eng. A* **2011**, *528*, 8286–8291. [CrossRef]

30. Cintas, J.; Montes, J.M.; Cuevas, F.G.; Herrera, E.J. Heat-resistant bulk nanostructured P/M aluminium. *J. Alloy. Compd.* **2008**, *458*, 282–285. [CrossRef]
31. Metal Powder Industries Federation. *Standard Test Method 10: Method for Determination of the Tensile Properties of Powder Metallurgy (PM) Materials*; Metal Powder Industries Federation: Princeton, NJ, USA, 2016.
32. Cintas, J.; Caballero, E.S.; Montes, J.M.; Cuevas, F.G.; Arevalo, C. Nanocrystalline Al composites from powder milled under ammonia gas flow. *Adv. Mater. Sci. Eng.* **2014**, *2014*, 1–8. [CrossRef]
33. Caballero, E.S.; Cintas, J.; Herrera-García, M.; Cuevas, F.G.; Montes, J.M. Order effect of vacuum and ammonia atmospheres on aluminium nitriding by mechanical alloying. *Mater. Sci. Forum* **2012**, *730–732*, 936–941. [CrossRef]
34. Young, R.A. *The Rietveld Method*; Oxford University Press: New York, NY, USA, 1995.
35. Bray, J.W. *ASM Handbooks Volume 2*; Specific Metals and Alloys: Properties of Wrought Aluminium Alloys; ASM International (American Society of Materials): Materials Park, OH, USA, 1990.